On the Asymptotic Convergence of *B*-Spline Wavelets to Gabor Functions

Michael Unser, *Member, IEEE*, Akram Aldroubi, and Murray Eden, *Life Fellow, IEEE*

***Abstract*—A family of nonorthogonal polynomial spline wavelet transforms is considered. These tranforms are fully reversible and can be implemented efficiently. The corresponding wavelet functions have a compact support. It is proven that these *B*-spline wavelets converge to Gabor functions (modulated Gaussian) pointwise and in all L_p-norms with $1 \le p < +\infty$ as the order of the spline (n) tends to infinity. In fact, the approximation error for the cubic *B*-spline wavelet ($n = 3$) is already less than 3%; this function is also near optimal in terms of its time/frequency localization in the sense that its variance product is within 2% of the limit specified by the uncertainty principle.**

***Index Terms*—Wavelet transform, Gabor transform, uncertainty principle, polynomial spline, *B*-splines, time-frequency localization.**

I. Introduction

There has been a recent growth in studies of time-frequency or multi-channel decompositions that allow a signal analysis to be localized in both time and frequency [1]–[3]. These representations constitute the natural mathematical tools for handling time-variant (or space-variant) signals. Hierarchical representations such as the wavelet transform also enable the characterization of a signal considered at different scales (multiresolution analysis) [4].

One of such decompositions is the Gabor transform by which a continuous time function is represented by a sum of elementary Gaussian signals [5], [6]:

$$g(x) = \sum_{m,n} a_{m,n} h_{m,n}(x). \tag{1.1}$$

The Gabor basis functions

$$h_{m,n}(x) = \exp\left(in\Omega(x - mT)\right) \frac{1}{\sqrt{2\pi}\, T_1} \cdot \exp\left(-\frac{(x - mT)^2}{2T_1^2}\right) \tag{1.2}$$

are obtained by modulation and translation of an elementary Gaussian pulse with a standard deviation T_1. The modulation and shift parameters Ω and T typically satisfy the constraints $\Omega T = 2\pi$ and $T = T_1$ [5]. One of the many advantages of Gabor functions is that they are optimally concentrated in both time and frequency domain. Typical applications are the time-frequency analysis of nonstationary signals [2] and image segmentation based on texture [7].

Another time-frequency representation is the recently proposed wavelet transform [3], [4], [8] by which a continuous-time function $g \in L_2$ is decomposed as

$$g(x) = \sum_{(k,i) \in Z^2} d_{(i)}(k) 2^{-i/2} \psi(2^{-i}x - k). \tag{1.3}$$

The corresponding basis functions are obtained by translation (index k) and dilation (index i) of a single prototype: the wavelet function ψ. One of the interesting properties of the wavelet transform is that it is relatively easy to construct a function $\mathring{\psi}$ that satisfies the biorthogonality condition

$$\langle \psi(2^{-i}x - k), \mathring{\psi}(2^{-j}x - l) \rangle = \begin{cases} 2^i & \text{for } (i = j) \text{ and } (k = l), \\ 0, & \text{otherwise}. \end{cases} \tag{1.4}$$

This function can be used to obtain the expansion coefficients by simple inner product

$$d_{(i)}(k) = \langle g(x), 2^{-i/2} \mathring{\psi}(2^{-i}x - k) \rangle. \tag{1.5}$$

In the case of an orthogonal wavelet transform, the biorthogonal function $\mathring{\psi}$ is equal to the wavelet itself. Although this inversion formula is simple conceptually, it is the algorithm recently proposed by S. Mallat that makes the wavelet transform particularly attractive [4]. The insight of Mallat was to relate an orthogonal wavelet transform with a multiresolution signal analysis by which a function is projected on a sequence of nested function spaces. This led him to derive a simple reversible algorithm using quadrature mirror filters (QMF) which is computationally very efficient.

One of the reasons for the popularity of the Gabor representation is the fact that the basis functions are optimal in terms of their time-frequency localization. However, the representation is redundant and the inversion of the transform can be unstable, especially when the product ΩT is close to 2π [3], [9]. The wavelet transform, on the other hand, is stable numerically and is intrinsically non-redundant (i.e., it is a one-to-one linear mapping). Another attractive feature is the hierarchical organization of its basis functions as opposed to the use of a fixed window size for the Gabor transform. In this correspondence, we will provide a further argument in favor of this type of representation by showing that there exists a class of wavelet tranforms for which the basis functions tend to modulated Gaussians, also suggesting that they exhibit near optimal time-frequency localization.

For this purpose, we will consider *B*-spline wavelets that are the natural counterparts of the classical *B*-splines; these wavelets were constructed independently by Chui and Wang, and Unser *et al.* [10], [11]. An essential property of these functions is their compact support. They are, therefore, much better localized in time than their orthogonal equivalents: the Battle/Lemarié polynomial spline wavelets [12], [13], which have an exponential decay. Another advantage of this representation is a simplification of the digital filters for the fast wavelet algorithm [11].

The presentation is organized as follows. Section II provides a summary of the main properties of the family of *B*-spline wavelet transforms. It also illustrates qualitatively the fact that piecewise linear and cubic *B*-spline wavelets are remarkably similar to their Gaussian approximations. Section III presents some preliminary mathematical results with an illustrative proof of the L_p-convergence of the standard *B*-splines to a Gaussian as n tends to infinity. Section IV develops the proof of the convergence of *B*-spline wavelets to modulated Gaussians as the order of the spline goes to infinity. It then briefly addresses the issue of time-frequency localization and presents some numerical performance indices.

Manuscript received March 1991; revised Setember 1991. This work was presented in part at the International Conference on Industrial and Applied Mathematics, Washington, DC, July 8–12, 1991.

The authors are with the Biomedical Engineering and Instrumentation Program, Building 13, Room 3W13, National Center for Research Resources, National Institutes of Health, Bethesda, MD 20892.

IEEE Log Number 9104596.

0018-9448/92$03.00

II. The B-Spline Wavelet Transform

A. Polynomial Spline Functions Spaces

A convenient way to introduce the B-spline wavelet transform is to consider a sequence of embedded polynomial spline function spaces $\{S^n_{(i)}, i \in Z\}$ of order $n = 2p + 1$ such that $S^n_{(i)} \supset S^n_{(i+1)}$ for $i \in Z$. $S^n_{(i)}$ is the subset of functions in L_2 that are of class C^{n-1} (i.e., continuous functions with continuous derivatives up to order $n - 1$) and are equal to a polynomial of degree n (odd) on each interval $[k \cdot 2^i, (k+1) \cdot 2^i]$ with $k \in Z$. An equivalent definition, adapted from Schoenberg [14], is

$$S^n_{(i)} = \left\{ g^n_{(i)}(x) = \sum_{k=-\infty}^{+\infty} c_{(i)}(k)\beta^n_{2^i}(x - 2^i k),\ (x \in R,\ d_{(i)} \in l_2) \right\} \tag{2.1a}$$

where $\beta^n_{2^i}(x) = \beta^n(x/2^i)$. The basis function $\beta^n(x)$ is the central B-spline of order n that can be generated by repeated convolution of a spline of order 0

$$\beta^n(x) = \beta^0 * \beta^{n-1}(x), \tag{2.1b}$$

where $\beta^0(x)$ is the indicator function in the interval $[-1/2, 1/2)$. This definition states that any polynomial spline function can be represented by a weighted sum of shifted B-splines and is therefore entirely characterized by its sequence of B-spline coefficients. The fundamental characteristic of B-spline basis functions is their compact support, the property that makes them useful in a variety of applications [15].

B. B-Spline Wavelet Transform

Given a function $g(x)$, we can obtain the B-spline representation (or approximation) at our finest resolution level that we arbitrarily define as level (0). Using (2.1), this function is represented in terms of its B-spline coefficients

$$g^n_{(0)}(x) = \sum_{k=-\infty}^{+\infty} c_{(0)}(k)\beta^n(x - k). \tag{2.2}$$

The essence of the wavelet transform is to decompose this expression using basis functions that are expanded by a factor of two

$$\begin{aligned} g^n_{(0)}(x) &= \sum_{k=-\infty}^{+\infty} d_{(1)}(k)\underline{\beta}^n_2(x - 2k) + \sum_{k=-\infty}^{+\infty} c_{(1)}(k)\beta^n_2(x - 2k) \\ &= \sum_{k=-\infty}^{+\infty} d_{(1)}(k)\underline{\beta}^n_2(x - 2k) + g^n_{(1)}(x), \end{aligned} \tag{2.3}$$

where $\underline{\beta}^n_2(x)$ is the B-spline wavelet defined by

$$\underline{\beta}^n_2(x) = \sum_{k=-\infty}^{+\infty} \tilde{b}^{2n+1} * \tilde{u}^n_2(k+1)\beta^n(x - k). \tag{2.4}$$

In this formula, $b^{2n+1}(k) := \beta^{2n+1}(k)$, u^n_2 is the binomial kernel of order $n = 2p + 1$:

$$u^n_2(k) = \begin{cases} \dfrac{1}{2^n}\dbinom{n+1}{k + (n+1)/2}, & |k| \le (n+1)/2, \\ 0, & \text{otherwise} \end{cases} \tag{2.5}$$

and "$*$" denotes the discrete convolution; the symbol "$\sim$" represents the modulation operator; i.e., $\tilde{a}(k) = (-1)^k a(k)$. The B-spline wavelet is a polynomial spline of compact support with the property that $\underline{\beta}^n_2(x) \perp \beta^n_2(x - 2k)$, $k \in Z$ (cf. [10], [11]). It follows that the first term of the right-hand side of (2.3) is the projection of $g^n_{(0)}$ on $S^n_{(1)}$ and the second term represents the residual error. The decomposition can be reapplied iteratively up to a depth I, which yields the wavelet representation

$$g^n_{(0)}(x) = \sum_{i=1}^{I} \sum_{k=-\infty}^{+\infty} d_{(i)}(k)\underline{\beta}^n_{2^i}(x - 2^i k) + \sum_{k=-\infty}^{+\infty} c_{(I)}(k)\beta^n_{2^I}(x - 2^I k), \tag{2.6}$$

where $\underline{\beta}^n_{2^i}(x) = \underline{\beta}^n_2(x/2^{i-1})$. The coefficients $\{d_{(1)}, \cdots, d_{(I)}\}$ are the so-called wavelet coefficients ordered from fine to coarse (their number is reduced by a factor of two for each increment of the resolution index) while the sequence $\{c_{(I)}\}$ characterizes the lower resolution signal at level (I). The wavelet transform provides a linear one-to-one mapping between the coefficients in (2.2) and (2.6), a process that is fully reversible. This decomposition can in principle be carried out over all resolution levels and yield a representation equivalent to (1.3) by taking $\psi(x) = \underline{\beta}^n(x) = \underline{\beta}^n_2(2x)$. It can be verified that the corresponding functions $\mathring{\underline{\beta}}^n(x)$ that satisfy the biorthogonality condition (1.4) are the dual spline wavelets

$$\mathring{\underline{\beta}}^n(x) = \sum_{k=-\infty}^{+\infty} \left(b^{2n+1} * [\tilde{b}^{2n+1} * b^{2n+1}]_{\downarrow 2}\right)^{-1}(k) \cdot \underline{\beta}^n(x - k), \tag{2.7}$$

which have been described in [11]. A different—but equivalent—definition of these dual wavelets is also given in [10]. These modified basis functions can be used to define the dual spline wavelet transform. This corresponds merely to interchanging the roles of the functions $\psi(x)$ and $\mathring{\psi}(x)$ in (1.3) and (1.5).

The B-spline basis functions at resolution level (1) for the piecewise linear ($n = 1$) and cubic ($n = 3$) spline transforms are shown in Fig. 1. Superimposed in dotted lines are the Gaussian approximations derived from Theorem 1 and 2 (cf. Sections III and IV)

$$\beta^n(x) \cong \sqrt{\frac{6}{\pi(n+1)}} \exp\left(-\frac{6x^2}{(n+1)}\right), \tag{2.8}$$

$$\beta^n(x) \cong \frac{4a^{n+1}}{\sqrt{2\pi(n+1)}}\sigma_w \cos(2\pi f_0(2x - 1)) \cdot \exp\left(-\frac{(2x-1)^2}{2\sigma_w^2(n+1)}\right), \tag{2.9}$$

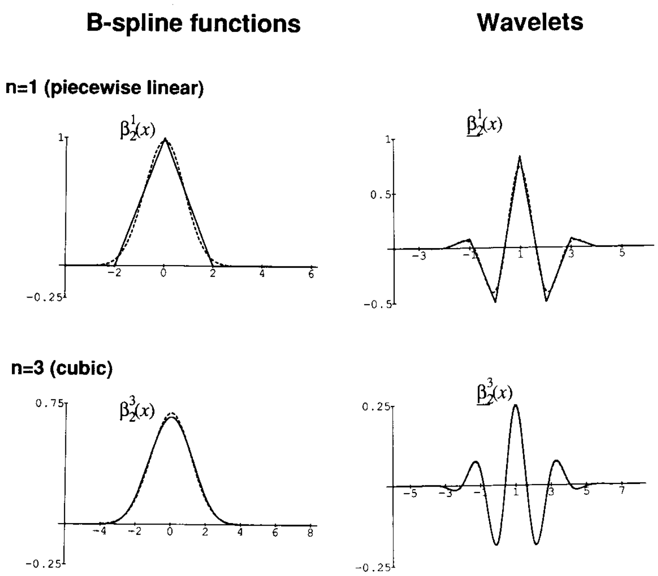

Fig. 1. Examples of B-spline basis functions and wavelets with their corresponding Gabor approximations (dotted lines) at resolution level (1).

with $a = 0.697066$, $f_0 = 0.409177$ and $\sigma_w^2 = 0.561145$. It can be seen from this graph that the quality of the approximation is already quite good for $n = 1$ and $n = 3$.

C. Fast Algorithm

To demonstrate the practicality of this approach, we succinctly describe a modified form of Mallat's QMF algorithm that allows an efficient evaluation of the direct and indirect B-spline wavelet transforms. The procedure usually starts with a sequence of sampled values $\{g(k)\}$ of the function $g_{(0)}^n(x)$ at resolution level 0. The initialization step involves the determination of the corresponding B-spline coefficients, performed by recursive filtering according to the procedure described in [16]

$$c_{(0)}(k) = (b^n)^{-1} * g(k),$$

where $(b^n)^{-1}$ denotes the convolution inverse of the discrete B-spline kernel $b^n(k) := \beta^n(k)$. The wavelet coefficients are then computed iteratively for $i = 0$ down to $I - 1$ by filtering and down-sampling by a factor of two

$$\begin{cases} c_{(i+1)}(k) = \left[v * c_{(i)}\right]_{\downarrow 2}(k) \\ d_{(i+1)}(k) = \left[\underline{v} * c_{(i)}\right]_{\downarrow 2}(k) \end{cases}, \quad (i = 1, \cdots, I - 1). \quad (2.10)$$

The indirect wavelet transform (reconstruction) is implemented in a similar fashion (upsampling and post-filtering) by successively reconstructing the B-spline coefficients starting at the bottom of the pyramid

$$d_{(i-1)}(k) = w * \left[c_{(i)}\right]_{\uparrow 2}(k) + \underline{w} * \left[d_{(i)}\right]_{\uparrow 2}(k), \quad (i = I, \cdots, 1). \quad (2.11)$$

At the very end of the procedure, the initial signal values are recovered by convolution with a sampled B-spline kernel

$$g(k) = b^n * c_{(0)}(k). \quad (2.12)$$

The expression for the filtering kernels in (2.10) and (2.11), which were derived in [11], are

$$\begin{cases} v(k) = \frac{1}{2}\left[(b^{2n+1})^{-1}\right]_{\uparrow 2} * b^{2n+1} * u_2^n(k) \\ \underline{v}(k+1) = \frac{1}{2}\left[(b^{2n+1})^{-1}\right]_{\uparrow 2} * \tilde{u}_2^n(k) \\ w(k) = u_2^n(k) \\ \underline{w}(k-1) = \tilde{b}^{2n+1} * \tilde{u}_2^n(k) \end{cases}. \quad (2.13)$$

We note that the synthesis filters have a finite impulse response that makes the reconstruction part of the algorithm quite efficient. Moreover, the analysis filters can be implemented recursively as suggested in [11]. In contrast with Mallat's QMF algorithm [4], the present analysis and synthesis filters are not identical and the filters in channel 0 and 1 are not modulated versions of each another. This disparity is a consequence of the nonorthogonality of the B-spline wavelet transform. The impulse responses of the filters for the cubic B-spline wavelet transform are given in Table I.

The dual spline wavelet transform can be computed using a similar algorithm by simply interchanging the analysis (v and $\underline{v}$) and synthesis filters (w and $\underline{w}$). The wavelet coefficients in this case correspond to the inner product between the signal $g(x)$ and B-spline wavelets (cf. (1.5)). The decomposition algorithm now uses a simple FIR filter bank which may be an asset in some computer vision applications such as edge detection or texture segmentation. There is also a direct link between this representation and a number of earlier multi-resolution techniques such as scale-

TABLE I
FIRST 14 COEFFICIENTS OF THE IMPULSE RESPONSES OF THE FILTERS FOR THE CUBIC B-SPLINE WAVELET TRANSFORM. ONLY b^3, w AND $\underline{w}$ ARE FIR

k	$(b^3)^{-1}(k)$	$b^3(k)$	$v(k)$	$\underline{v}(k+1)$	$w(k)$	$\underline{w}(k-1)$
0	+1.732	+4/6	+0.8932	+1.475	+0.75	+0.6018
−1, 1	−0.4641	+1/6	+0.4007	−0.4684	+0.5	−0.4584
−2, 2	+0.1244		−0.2822	−0.7421	+0.125	+0.196
−3, 3	−0.03332		−0.2329	+0.3458		−0.04159
−4, 4	+0.008928		+0.1291	+0.3897		+0.003075
−5, 5	−0.002392		+0.1265	−0.1968		0.0000248
−6, 6	+0.000641		−0.06642	−0.2077		
−7, 7	−0.0001718		−0.0679	+0.1068		
−8, 8	···		+0.03523	+0.1111		
−9, 9			+0.03637	−0.05733		
−10, 10			−0.01882	−0.05943		
−11, 11			−0.01947	+0.03071		
−12, 12			+0.01007	+0.03181		
−13, 13			+0.01042	−0.01644		

space filtering [17] and the Gaussian pyramid [18]; this issue is further discussed in [19].

III. PRELIMINARY RESULTS

We now turn to the issue of the convergence of the B-spline wavelets to Gaussian signals. For this purpose, we first need to establish some preliminary results that will play a crucial role in the proof in section IV.

A. A Convergence Result

Lemma 1: Let $A(x)$ be a function with a positive maximum at $x = x_0$ such that:

a) $A(x_0) > 0$

b) $\left.\dfrac{\partial A(x)}{\partial x}\right|_{x=x_0} = 0$

c) $-\infty < \left.\dfrac{\partial^2 A(x)}{\partial x^2}\right|_{x=x_0} = -\alpha^2 A(x_0) < 0,$

and consider the sequence

$$A_n(x) = \left[\frac{1}{A(x_0)} A\left(\frac{x}{\alpha} + x_0\right)\right]^n. \tag{3.1}$$

Then the limiting form of $A_n(x)$ as n tends to infinity is a Gaussian

$$\lim_{n\to+\infty} \{A_n(x/\sqrt{n})\} = \exp(-x^2/2). \tag{3.2}$$

We note that this result is closely related to the well known Central Limit Theorem [20], [21]. In this latter context, $A(x)$ is the characteristic function of a random variable (i.e., the Fourier transform of its probability density function) and has a maximum at $x = 0$.

Proof: For a fixed value of x, we consider the function

$$L_n(x) = \log A_n(x/\sqrt{n}) = n \log A_1(x/\sqrt{n}).$$

To evaluate the limit

$$\lim_{n\to+\infty} L_n(x) = \lim_{n\to+\infty} (n \log A_1(x/\sqrt{n})) = \lim_{n\to+\infty}\left(\frac{\log A_1(x/\sqrt{n})}{n^{-1}}\right),$$

we apply l'Hôpital's rule and differentiate twice to get

$$\lim_{n\to+\infty} L_n(x) = \lim_{n\to+\infty}\left(\frac{\frac{1}{2}n^{-3/2} \times A_1'(n^{-1/2}x)}{A_1(n^{-1/2}x)n^{-2}}\right) = \lim_{n\to+\infty}\left(\frac{x^2}{2} A_1''(n^{-1/2}x)\right) = -\frac{x^2}{2}.$$

We then use the fact that the inverse function $\exp(x)$ is continuous at $x = 0$, which finally yields (3.2). □

B. An Upper Bound for Standardized Sinc Functions

Lemma 2: For $n \in N$ and $n \geq 2$, the function $|\operatorname{sinc}(x/\sqrt{n})|^n$ is uniformly bounded from above by an $L_p(-\infty, +\infty)$ function $\kappa(x)$ where $p \in [1, +\infty)$

$$|\operatorname{sinc}(x/\sqrt{n})|^n \leq \kappa(x) = (1 - \operatorname{rect}[x/2])\frac{2}{(\pi x)^2} + \exp(-x^2). \tag{3.3}$$

Proof: We start with the inequality

$$\forall x \in [0, 1], \quad \operatorname{sinc}(x) \leq 1 - x^2,$$

where the right-hand side term is the parabola that goes through the two extreme values of sinc(x) within this interval. We will first show that

$$\forall x \in [-\sqrt{n}, \sqrt{n}],$$

$$\operatorname{sinc}^n(x/\sqrt{n}) \leq \left(1 - \frac{x^2}{n}\right)^n \leq \exp(-x^2). \tag{3.4}$$

For this purpose, we define the positive function

$$p(x) = \exp(x^2)\left(1 - \frac{x^2}{n}\right)^n.$$

The derivative of $p(x)$ is given by

$$\frac{\partial p(x)}{\partial x} = \frac{-2\exp(x^2)x^3(1 - x^2/n)^n}{n(1 - x^2/n)},$$

and is always negative for $x \in [0, \sqrt{n}]$. Therefore, the maximum of $p(x)$ within the interval occurs at $x = 0$

$$\sup_{x \in (0, \sqrt{n})} p(x) = p(0) = 1,$$

which proves (3.4). Second, we note that $|sinc(x/\sqrt{n})|^n$ is also bounded by

$$|\text{sinc}(x/\sqrt{n})|^n \leq \left(\frac{\sqrt{n}}{\pi x}\right)^n.$$

For $x \geq \sqrt{n}$ and $n \geq 2$, we get a bound that is independent of n by noticing that

$$\forall x \in (\sqrt{n}, +\infty) \qquad |\text{sinc}(x/\sqrt{n})|^n \leq \left(\frac{\sqrt{n}}{\pi x}\right)^n \leq \frac{2}{(\pi x)^2}. \tag{3.5}$$

Finally, we define the function $\kappa(x)$, which is independent of n, by suitably combining the right-hand sides of (3.4) and (3.5). □

C. Convergence of the B-Spline Functions

The well-known convolution property of B-splines suggests that these functions converge to a Gaussian as the order of the spline n tends to infinity. Here, we provide a proof for the general L_p convergence in both the frequency and time domain. The derivation is simple and provides an illustration of the use of Lemma 1 and 2. It also serves as a preparation of the proof for the convergence of wavelet functions presented in Section IV.

Theorem 1: The B-spline function $\beta^n(x)$ and its Fourier transform $B^n(f)$ both converge to a Gaussian as n tends to infinity:

$$\lim_{n \to +\infty}\left\{\sqrt{\frac{n+1}{12}} \times \beta^n\left(\sqrt{\frac{n+1}{12}}\,x\right)\right\} = \frac{1}{\sqrt{2\pi}}\exp(-x^2/2), \tag{3.6}$$

$$\lim_{n \to +\infty}\left\{B^n\left(\frac{f}{2\pi}\sqrt{\frac{12}{n+1}}\right)\right\} = \exp(-f^2/2). \tag{3.7}$$

Moreover, $B^n(f/\sqrt{\pi^2(n+1)/3})$ converge to $\exp(-f^2/2)$ in $L_p(-\infty, +\infty)\ \forall p \in [1, +\infty)$, and $\sqrt{(n+1)/12}\ \beta^n(\sqrt{(n+1)/12} \cdot x)$ converge to $\exp(-x^2/2)/\sqrt{2\pi}$ in $L_q(-\infty, +\infty) \forall q \in [2, +\infty]$, as n goes to infinity.

Proof: The Fourier Transform of a B-spine of order n is given by

$$\beta^n(x) \quad \overset{Fourier}{\longleftrightarrow} \quad B^n(f) = \text{sinc}^{n+1}(f). \tag{3.8}$$

Clearly, $B^0(f) = \text{sinc}(f)$ has a maximum at $f = 0$ and satisfies all the conditions in Lemma 1. Its second derivative at $f = 0$ can be written as

$$\left.\frac{\partial^2 B^0(f)}{\partial f^2}\right|_{f=0} = -\alpha^2 = -\frac{\pi^2}{3} = -(2\pi)^2\sigma_0^2, \tag{3.9}$$

where $\sigma_0^2 = 1/12$ is the variance of the zero order spline: $\beta^0(x) = \text{rect}(x)$. Therefore, we have that

$$\lim_{n \to +\infty}\left\{B^n\left(\frac{f}{2\pi\sigma_0\sqrt{n+1}}\right)\right\} = \exp(-f^2/2),$$

which proves the pointwise convergence. Clearly, $B^n(f/\alpha)$ is bounded by the L_p function $\kappa(f/\alpha)$ defined in Lemma 2 and this bound is independent of n. The use of Lebesgue's dominated convergence Theorem provides the L_p convergence for $p \in [1, +\infty)$. The L_q convergence with $q \in [2, +\infty]$ in the time domain follows as a consequence of Titchmarsh inequality, which states that for $1 \leq p \leq 2$ and $p^{-1} + q^{-1} = 1$, the Fourier transform is a bounded linear operator from $L_p(-\infty, +\infty)$ into $L_q(-\infty, +\infty)$. □

IV. Convergence of the B-Spline Wavelets

A. The Main Convergence Theorem

We first define the centered (and symmetrical) B-spline wavelet of order n

$$\gamma_2^n(x) := \underline{\beta}_2^n(x-1) \quad \overset{Fourier}{\longleftrightarrow} \quad G_2^n(f) = |\underline{B}_2^n(f)| \tag{4.1}$$

and the auxiliary function

$$C(f) := \frac{1}{2}\left[\frac{\sin 2\pi(f - \frac{1}{2})}{\sin \pi(f - \frac{1}{2})}\right]\text{sinc}(f)\,\text{sinc}^2\left(f - \frac{1}{2}\right) = \frac{1}{4}\frac{\sin^2(2\pi f)}{4\pi^3 f(f - \frac{1}{2})^2}. \tag{4.2}$$

Theorem 2: The Fourier transforms of centered B-spline wavelets of order n converge to a Gaussian, as n tends to infinity

$$\lim_{n \to +\infty}\left\{\frac{1}{2(C(f_0))^{n+1}}\,G_2^n\left(\frac{f}{2\pi\sigma_w\sqrt{n+1}} \pm f_0\right)\right\} = \exp(-f^2/2), \tag{4.3}$$

where the modulation and dispersion parameters f_0 and σ_w are given by

$$f_0 = \arg\max_{f\in R} \{C(f)\} \cong 0.409177 \quad (4.4a)$$

$$\sigma_w^2 = \frac{-\left.\dfrac{\partial^2 C(f)}{\partial f^2}\right|_{f=f_0}}{C(f_0)(2\pi)^2} \cong 0.561145. \quad (4.4b)$$

Moreover, the standardized L_p and L_q-norms of the corresponding approximation errors in the frequency and time domain also tend to zero

$$\lim_{n\to+\infty}\left\| \frac{1}{2(C(f_0))^{n+1}} G_2^n\left(\frac{f}{2\pi\sigma_w\sqrt{n+1}}\right) - \exp\left(-\frac{(f-f_0 2\pi\sigma_w\sqrt{n+1})^2}{2}\right)\right\|_{L_p(0,+\infty)} = 0$$

$$\lim_{n\to+\infty}\left\| \frac{\sigma_w\sqrt{n+1}}{4(C(f_0))^{n+1}} \gamma_2^n((\sigma_w\sqrt{n+1})x) - \frac{\cos(2\pi f_0(\sigma_w\sqrt{n+1})x)}{\sqrt{2\pi}}\exp\left(-\frac{x^2}{2}\right)\right\|_{L_q(-\infty,+\infty)} = 0$$

for $p\in[1,+\infty)$ and $q\in[2,+\infty]$, respectively.

B. Proof

The Fourier transform of the centered B-spline wavelet is given by

$$G_2^n(f) = \frac{2}{2^{n+1}}\left[\frac{\sin 2\pi(f-\frac{1}{2})}{\sin\pi(f-\frac{1}{2})}\right]^{n+1}\operatorname{sinc}^{n+1}(f) \cdot \sum_{k=-\infty}^{+\infty}\operatorname{sinc}^{2n+2}\left(f-\frac{1}{2}-k\right), \quad (4.5)$$

which can also be decomposed as

$$G_2^n(f) = 2(C(f))^{n+1} + R^n(f), \quad (4.6)$$

where $C(f)$ is defined by (4.2) and where the residue $R^n(f)$ is given by

$$R^n(f) = \frac{2}{2^{n+1}}\frac{\sin^{n+1}(2\pi(f-\frac{1}{2}))}{\sin^{n+1}(\pi(f-\frac{1}{2}))}\operatorname{sinc}^{n+1}(f) \cdot\left\{\sum_{k=1}^{-\infty}\operatorname{sinc}^{2n+2}\left(f-\frac{1}{2}-k\right) + \operatorname{sinc}^{2n+2}\left(f-\frac{1}{2}+k\right)\right\}.$$

The proof consists of two main parts. The first will be to examine the convergence of $(C(f))^{n+1}$ and the second will be to show that the residue converges to zero. We note that the derivation is only concerned with the positive part of the frequency axis. The same arguments can be used to obtain the convergence on the negative axis because

$$G_2^n(f) = G_2^n(-f) = 2(C(-f))^{n+1} + R^n(-f).$$

Convergence of $(C(f))^{n+1}$: The graph of the function $C(f)$ is given in Fig. 2. It is not difficult to show that $C(f)$ has a global maximum that occurs in the interval (0, 1). To find it, we take the first derivative

$$\frac{\partial C(f)}{\partial f} = \frac{\sin(2\pi f)}{\pi^3 f^2(2f-1)^3} \cdot(\cos(2\pi f)(8\pi f^2 - 4\pi f) - \sin(2\pi f)(6f-1))$$

and set this expression to zero. The maximum occurs at $f_0 = 0.409177$, which is the solution of

$$\cos(2\pi f_0)(8\pi f_0^2 - 4\pi f_0) - \sin(2\pi f_0)(6f_0-1) = 0 \quad (4.7)$$

The second derivative at $f=f_0$ is negative and can be written as

$$\left.\frac{\partial^2 C(f)}{\partial f^2}\right|_{f=f_0} = -C(f_0)(2\pi)^2\sigma_w^2,$$

where $C(f_0) = 0.697066$ and $\sigma_w^2 = 0.561145$. Since $\partial C(f)/\partial f$ is zero at $f=f_0$, we can use Lemma 1 to show that $(C(f))^{n+1}$ converges pointwise to a shifted Gaussian

$$\lim_{n\to+\infty}\left\{\frac{1}{a^{n+1}}\left(C\left(\frac{f}{b\sqrt{n+1}}+f_0\right)\right)^{n+1}\right\} = \exp(-f^2/2),$$

where $a = C(f_0)$ and $b = 2\pi\sigma_w$ are two proper scaling constants. The next step is to establish the two following inequalities

$$\frac{1}{a}C(f+f_0) \le 1 - f^2, \qquad \text{for } f\in(-1,1),$$
$$\frac{1}{a}C(f+f_0) \le \frac{1}{\pi f}, \qquad \text{for } |f|\in(1,+\infty),$$

and to use the same technique as in Section II-B in order to prove that

$$\frac{1}{a^n}C\left(\frac{f}{b\sqrt{n}}+f_0\right)^n \le \kappa\left(\frac{f}{b}\right), \qquad \text{for } f\in R \text{ and } n\ge 2, \quad (4.8)$$

where $\kappa(f)$ is the function defined in Lemma 2. Since $\kappa(f)\in L_p(-\infty,+\infty)$ with $p\in[1,+\infty)$, we then use Lebesgue's dominated convergence Theorem to obtain the L_p convergence for $p\in[1,+\infty)$.

Convergence of the Residue: First we rewrite $R^n(f)$ in the

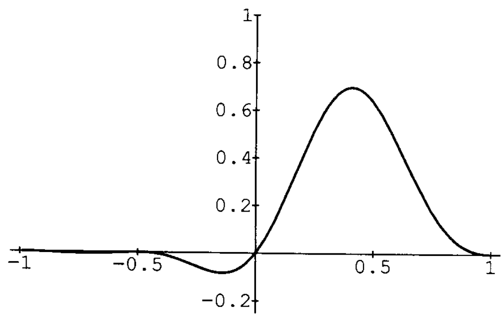

Fig. 2. Graph of the function $C(f)$.

more convenient form

$$R^n(f) = 2\sin^{n+1}(\pi f)\,\mathrm{sinc}^{n+1}(f)S^{2n+1}\left(f - \tfrac{1}{2}\right), \quad (4.9)$$

where

$$S^{2n+1}(f) = \sum_{k=1}^{+\infty} \mathrm{sinc}^{2n+2}(f-k) + \mathrm{sinc}^{2n+2}(f+k). \quad (4.10)$$

We also need an upper bound for the function $S^{2n+1}(f)$, which is provided by the following result.

Lemma 3: The symmetrical function $|S^{2n+1}(f)|$ is bounded from above

$$\forall f \in (0,1), \quad |S^{2n+1}(f)| < \frac{4}{\pi^{2n+2}(1-f)^{2n+2}} \quad (4.11)$$

and

$$\forall f \in (0,+\infty), \quad |S^{2n+1}(f)| \le 1. \quad (4.12)$$

Proof: To prove (4.11), we note that

$$\forall f \in \left(0, \frac{1}{2}\right), \quad |S^{2n+1}(f)| < 2\sum_{k=1}^{+\infty} \mathrm{sinc}^{2n+2}(f-k) \le \frac{2}{\pi^{2n+2}} \sum_{k=1}^{+\infty} (k-f)^{-2n-2}. \quad (4.13)$$

The sum that appears in the right hand side of this inequality can be bounded as

$$\sum_{k=1}^{+\infty} (k-f)^{-2n-2} \le (1-f)^{-2n-2} + \int_1^{+\infty} (x-f)^{-2n-2}\,dx, \quad (4.14)$$

where the integral is evaluated as

$$\int_1^{+\infty} (x-f)^{-2n-2}\,dx = \frac{1}{(2n+1)(1-f)^{2n+1}} = \frac{1}{(1-f)^{2n+2}} \frac{(1-f)}{(2n+1)} < \frac{1}{(1-f)^{2n+2}}. \quad (4.15)$$

By substituting (4.15) and (4.14) and replacing this expression in (4.13), we finally get (4.11). In order to prove the second part of the Lemma, we consider the function $B_1^{2n+1}(f) = S^{2n+1}(f) + \mathrm{sinc}^{2n+2}(f) \ge S^{2n+1}(f)$, which corresponds to the Fourier transform of the discrete B-spline kernel b^{2n+1}. We then use the norm inequality

$$|B_1^{2n+1}(f)| \le \|B_1^{2n+1}\|_\infty \le \|b^{2n+1}\|_{l_1}.$$

Since the B-splines are positive, we have that $\|b^{2n+1}\|_{l_1} = B_1^{2n+1}(0) = 1$, which provides the desired result. □

The task is now to find an upper bound for $R^{n-1}(f/(b\sqrt{n}))/a^n$ and to show that this bound converges to zero. For this purpose, we divide the frequency axis in two distinct intervals.

a) $f \in (0, b\sqrt{n})$: In this case, we have $|f/(b\sqrt{n}) - 1/2| < 1/2$ and we use the first part of Lemma 3 together with (4.9) to obtain

$$\forall f \in (0, b\sqrt{n}), \quad \left|\frac{1}{a^n} R^{n-1}\left(\frac{f}{b\sqrt{n}}\right)\right| < \frac{8}{a^n} \sin^n\left(\frac{\pi f}{b\sqrt{n}}\right) \mathrm{sinc}^n\left(\frac{f}{b\sqrt{n}}\right) \cdot \left(\frac{1}{\pi\left(1 - \left|\frac{1}{2} - f/(b\sqrt{n})\right|\right)}\right)^{2n}.$$

If we define the constant $c = \max\{\sin(\pi x)\,\mathrm{sinc}(x)\}/a = 1.03952$, we also have that

$$\forall f \in (0, b\sqrt{n}), \quad \left|\frac{1}{a^n} R^{n-1}\left(\frac{f}{b\sqrt{n}}\right)\right| < 8c^n\left(\frac{1}{\pi\left(1 - \left|\frac{1}{2} - f/b\sqrt{n}\right|\right)}\right)^{2n} < 8\left(\frac{2\sqrt{c}}{\pi}\right)^{2n},$$

which clearly converges to zero as n goes to infinity. We can also get an estimate of the L_p-norm by taking the integral

$$\left\|\frac{1}{a^n} R^{n-1}\left(\frac{f}{b\sqrt{n}}\right)\right\|^p_{L_p(0,b\sqrt{n})} < \left(\frac{8^p c^{pn}}{\pi^{2pn}}\right) \times 2b\sqrt{n} \int_0^{1/2} \frac{dx}{(1-x)^{2np}} = 2(b\sqrt{n})\left(\frac{8^p c^{pn}}{\pi^{2pn}}\right) \frac{2^{2np-1} - 1}{2np - 1}.$$

This inequality can be manipulated to yield

$$\left\| \frac{1}{a^n} R^{n-1}\left(\frac{f}{b\sqrt{n}}\right)\right\|^p_{L_p(0,b\sqrt{n})} < b8^p\left(\frac{4c}{\pi^2}\right)^{np}. \quad (4.16)$$

Since $4c/\pi^2 < 1$, this expression also converges to zero as n tends to infinity.

b) $f \in (b\sqrt{n}, +\infty)$: For this interval, we note that $R^n(f)$ is bounded by $2\ |\text{sinc}(f)|^{n+1}$. Therefore, we have that

$$\forall f \in (b\sqrt{n}, +\infty), \quad \left|\frac{1}{a^n} R^{n-1}\left(\frac{f}{b\sqrt{n}}\right)\right| < \frac{2}{a^n}\left(\frac{n^{1/2}b}{\pi f}\right)^n < 2\left(\frac{1}{a\pi}\right)^n,$$

which converges to zero as n goes to infinity. An estimate of the corresponding L_p-norm is given by

$$\left\| \frac{1}{a^n} R^{n-1}\left(\frac{f}{b\sqrt{n}}\right)\right\|^p_{L_p(b\sqrt{n},+\infty)} < \int_{b\sqrt{n}}^{+\infty} 2^p\left(a\pi f/b\sqrt{n}\right)^{-2pn} df = \frac{b2^p\sqrt{n}}{(a\pi)^{2pn}(2np-1)}, \quad (4.17)$$

which also tends to zero as n goes to infinity.

We then complete the proof by observing that the pointwise convergence of both $(C(f))^n$ and $R^n(f)$ on the positive frequency axis implies the pointwise convergence of $G_2^n(f)$ to a shifted Gaussian as specified in (4.3). Moreover, we use the fact that the L_p-norm of the global residual error is bounded by the sum of the individual L_p-norms in (4.16) and (4.17), plus the contribution due to $(C(f))^n$, which implies the $L_p(0, +\infty)$ convergence in the Fourier domain with $p \in [1, +\infty)$. The same result obviously also holds for the negative part of the frequency axis since the function $G_2^n(f)$ is symmetrical. Finally, we use the conjugacy property of the Fourier transform to obtain the L_q convergence in the time domain with $q \in [2, +\infty]$. □

C. Optimal Time-Frequency Localization

Let us consider an arbitrary function $g(x)$ with its Fourier transform $G(f)$. The uncertainty principle sets a lower limit $(2\pi)^{-2}$ on the product of the variances (or uncertainties) in the time (σ_x^2) and frequency domain (σ_f^2) [5]. This product is known to be minimum for the class of Gaussian functions including modulated Gaussians of the form given by (1.2). Note that J. Morlet used such Gabor functions to define an integral wavelet transform that he used for the analysis seismic signals [1], [22].

In the proceding sections, we have demonstrated the Gaussian convergence of the functions $\beta^n(x)$ and $\underline{\beta}^n(x)$ as the order of the spline goes to infinity. In fact, the modulated Gaussian (2.9) corresponds to the real part of a Gabor function. These convergence results would also suggest near optimal behavior in terms of time-frequency localization. We have performed some numerical computations of the approximation errors and dispersion measures. These results, obtained by numerical integration, are summarized in Table II. Since the limiting form of the bandpass functions $\underline{B}^n(f)$ is in fact the superposition of two Gaussian functions at f_0 and $-f_0$, we have used a modified one-sided definition of the dispersion in the frequency domain in which the integrals are evaluated on the positive part of the frequency axis only. The quality of the approximation was measured by the relative root mean square error ϵ. These computations clearly indicate that, in accordance with our theoretical results, the approximation error decreases with n. The product of the time and frequency variances also seems to decrease with n. We note that for $n = 3$, it is already surprisingly close to the optimal limit for Gaussian functions. The largest uncertainty product occurs for the linear B-spline wavelet and can be attributed to a comparatively poor localization in the frequency domain, a consequence of the higher frequency components of $G_2^1(f)$ which decay like $O(1/f^2)$. For higher order splines, the decay at infinity is at least $O(1/f^{n+1})$ and this effect become less and less significant. In fact, our numerical results tend to support the conclusion that the localization performance of the cubic spline wavelet transform should be sufficient for most practical applications.

TABLE II
TIME/FREQUENCY LOCALIZATION AND APPROXIMATION ERROR FOR LOWER ORDER B-SPLINE BASIS FUNCTIONS AND WAVELETS

Function	ϵ	σ_x^2	$\bar{f}$	σ_f^2	$\sigma_x^2 \cdot \sigma_f^2 \cdot (4\pi)^2$
B-splines:					
$\beta^1(x)$	0.08916	0.1	0	0.07484	1.182
$\beta^3(x)$	0.03444	0.1806	0	0.03523	1.005
Wavelets:					
$\underline{\beta}_2^1(x)$	0.1065	0.6075	0.4235	$2.807\ 10^{-2}$	2.698
$\underline{\beta}_2^3(x)$	0.02677	1.1747	0.4109	$5.494\ 10^{-3}$	1.019

REFERENCES

[1] A. Grossmann and J. Morlet, "Decomposition of Hardy functions into square integrable wavelets of constant shape," *SIAM J. Math. Anal.*, vol. 15, pp. 723-736, July 1984.
[2] P. Flandrin, "Some aspects of non-stationary signal processing with emphasis on time-frequency and time-scale methods," in *Wavelets: Time-frequency methods and phase space*, J. M. Combes, A. Grossmann and P. Tchamitchian, New York: Springer-Verlag, 1989, pp. 68-98.
[3] I. Daubechies, "The wavelet transform, time-frequency localization and signal analysis," *IEEE Trans. Inform. Theory*, vol. 36, pp. 961-1005, Sept. 1990.
[4] S. G. Mallat, "A theory of multiresolution signal decomposition: the wavelet representation," *IEEE Trans. Pattern Anal. Machine Intell.*, vol. PAMI-11, pp. 674-693, 1989.
[5] D. Gabor, "Theory of communication," *J. Inst. Elect. Eng.*, vol. 93, pp. 429-457, 1946.
[6] M. J. Bastiaans, "Gabor's expansion of a signal into Gaussian elementary signals," *Proc. IEEE*, vol. 68, pp. 538-539, Apr. 1980.
[7] M. R. Turner, "Texture discrimination by Gabor functions," *Bio. Cybern.*, vol. 55, pp. 71-82, 1986.
[8] Y. Meyer, *Ondelettes et Opérateurs I: Ondelettes*. Paris, France: Hermann, 1990.
[9] A. J. E. M. Janssen, "Gabor representation of generalized functions," *J. Math. Appl.*, vol. 80, pp. 377-395, 1981.
[10] C. K. Chui and J. Z. Wang, "On compactly supported spline wavelets and a duality principle," CAT rep. 213, Texas A&M Univ., 1990 (to appear in *Trans. Am. Math. Soc.*).
[11] M. Unser, A. Aldroubi, and M. Eden, "A family of polynomial spline wavelet transforms," NCRR rep. 153/90, Nat. Inst. Health, 1990.
[12] P.-G. Lemarié, "Ondelettes à localisation exponentielles," *J. Math. pures et appl.*, vol. 67, pp. 227-236, 1988.
[13] G. Battle, "A block spin construction of ondelettes. Part I: Lemarié functions," *Commun. Math. Phys.*, vol. 110, pp. 601-615, 1987.
[14] I. J. Schoenberg, "Cardinal interpolation and spline functions," *J. Approx. Theory*, vol. 2, pp. 167-206, 1969.

[15] P. M. Prenter, *Splines and Variational Methods*. New York: Wiley, 1975.
[16] M. Unser, A. Aldroubi, and M. Eden, "Fast B-spline transforms for continuous image representation and interpolation," *IEEE Trans. Pattern Anal. Machine Intell.*, vol. 13, pp. 277-285, Mar. 1991.
[17] A. P. Witkin, "Scale-space filtering," in *Proc. 4th Int. Joint Conf. Artificial Intell.*, 1983, pp. 1019-1022.
[18] P. J. Burt and E. H. Adelson, "The Laplacian pyramid as a compact code," *IEEE Trans. Commun.*, vol. COM-31, pp. 337-345, Apr. 1983.
[19] M. Unser, A. Aldroubi, and M. Eden, "The L_2 polynomial spline pyramid: A discrete multiresolution representation of continuous signals," *IEEE Trans. Pattern Anal. Mach. Intell.*, accepted for publication.
[20] J. W. Lindeberg, "Eine neue Herleitung des Exponentialgesetzes in der Warhscheinlichkeitsrechnung," *Math. Zeit.*, vol. 15, pp. 211-235, 1922.
[21] W. Feller, *An Introduction to Probability Theory and Its Application. Vol. II.* New York: Wiley, 1971.
[22] J. Morlet, G. Arens, I. Fourgeau, and D. Giard, "Wave propagation and sampling theory," *Geophys.*, vol. 47, pp. 203-236, 1982.

On the Regularity of Wavelets

Hans Volkmer

***Abstract*—The regularity index α_N of the scaling functions ${}_N\phi$, $N = 2, 3, \cdots$ of multiresolution analysis introduced by Daubechies in 1988 is investigated. It is shown that $0.51 < \alpha_2 < 0.53$ and $\lim_{N\to\infty}\alpha_N/N = 1 - \log 3/(2\log 2)$.**

***Index Terms*—Wavelets, regularity index, dilation equation, Fourier transform, scaling functions.**

I. Introduction

If f is a trigonometric polynomial with $f(0) = 1$ then the infinite product

$$F(z) = \prod_{j=1}^{\infty} f(2^{-j}z) \tag{1.1}$$

defines an entire function F (e.g., see [6, Lemma 2.3]). In the special case $f(z) = \cos z$ we obtain

$$\prod_{j=1}^{\infty} \cos(2^{-j}z) = \frac{\sin z}{z}. \tag{1.2}$$

This method is used in [2] to solve dilation equations of multiresolution analysis by functions with compact support. The solutions (called scaling functions) are Fourier transforms of infinite products of the type previous shown. Then wavelet bases of $L^2(\boldsymbol{R})$ can be defined in terms of these scaling functions. One is interested to find scaling functions with compact support as smooth as possible which then leads to the problem to investigate the behavior of F for $\boldsymbol{R} \ni z \to \pm\infty$. In this correspondence, we treat this problem for the special trigonometric polynomials $f = f_N$, $N \in \boldsymbol{N}$, given in [2, Section 4]. These polynomials are products

$$f_N(z) = \left(\tfrac{1}{2}(1 + e^{iz})\right)^N g_N(z),$$

where g_N is a trigonometric polynomial satisfying $g_N(0) = 1$ and

$$|g_N(z)|^2 = P_N\left(\sin^2\left(\tfrac{1}{2}z\right)\right),$$

where

$$P_N(y) := \sum_{j=0}^{N-1} \binom{N-1+j}{j} y^j. \tag{1.3}$$

Here and in the following the arguments of our functions are always real numbers. The function g_N can be made unique by additional conditions which, however, are not needed in this correspondence because we only use $|g_N(z)|$. If we denote the functions of (1.1) corresponding to f_N, g_N by F_N and G_N, respectively, then (1.2) shows that

$$|F_N(z)| = \left|\frac{\sin\left(\frac{1}{2}z\right)}{\frac{1}{2}z}\right|^N |G_N(z)|. \tag{1.4}$$

As in [2, p. 981, (4.28)] (there is a misprint in that formula: the power $1 + \alpha$ has to be replaced by α), let α_N (the "regularity index" of the Fourier transform of F_N) be the supremum of all β such that

$$\int_{-\infty}^{\infty} (1 + |t|)^{\beta} |F_N(t)|\, dt < \infty. \tag{1.5}$$

Then the problem is to find upper and lower bounds of α_N. For instance, it is known that $\alpha_2 \geq 0.5$ (see [2, p. 984]). In Section III, we improve this to

$$0.51 < \alpha_1 < 0.53. \tag{1.6}$$

In a remark on p. 984 of [2] we find the value $\alpha_2 = 2 - (\log(1 + \sqrt{3}))/(\log 2) = 0.55 \cdots$. According to [3] this value corresponds to a different definition of the regularity index α_2. There α_2 is the supremum of all α such that the Fourier transform of F_2 belongs to the space Lip-α of functions f satisfying $|f(x) - f(x + t)| \leq C(1 + |t|)^{\alpha}$.

In particular, one is interested in the asymptotic behavior of α_N as N tends to infinity. It is known that $\alpha_N/N \geq 0.1936 + \mathcal{O}(N^{-1}\log N)$, see [2, p. 983]. However, the limit of α_N/N given on p. 983 of [2] has turned out to be wrong [3]. In Section IV of this paper, we will prove that

$$\lim_{n\to\infty} \frac{\alpha_N}{N} = 1 - \frac{\log 3}{2\log 2}. \tag{1.7}$$

Manuscript received December 20, 1991; revised May 25, 1991.
The author is with the Department of Mathematical Sciences, University of Wisconsin-Milwaukee, P.O. Box 413, Milwaukee, WI 53201.
IEEE Log Number 9105029.